Electronic Supplementary Material (ESI) for Dalton Transactions.

A Lanthanide-tellurium heterometal encapsulated sandwich-type heteropolyoxoniobate with a 3D *pcu*-type hydrogen -bonding network

Rong-Da Lai, Hui-Lin Feng, Yan-Qiong Sun*, Xin-Xiong Li and Shou-Tian Zheng*

College of Chemistry, Fuzhou University, Fuzhou, Fujian 350108, China.

This file includes:

Section 1: Experimental Section

Materials and General Methods. Except that $K_7H[Nb_6O_{19}]\cdot 13H_2O$ precursor was synthesized according to a literature method and confirmed by IR spectra.[19] All chemicals were commercially purchased and directly used without further purification. Elemental analyses of C, H and N were carried out with a Vario MICRO elemental analysis. IR spectra were recorded on an Opus Vertex 70 FT-IR infrared spectrophotometer in the range of 400 - 4000 cm^{-1}. Thermogravimetric analysis was performed on a Mettler Toledo TGA/SDTA 851e analyzer under an air-flow atmosphere with a heating rate of 10 ºC/min in the temperature of 30-750 ºC. Powder X-ray diffraction (PXRD) patterns were measured using a Rigaku DMAX 2500 diffractometer with CuKα radiation (λ = 1.5418 Å). UV-vis absorption spectra were collected using a PerkinElmer Lambda 35 spectrophotometer to monitor the release process.

Synthesis of $H_5[Cu(H_2O)(en)_2]_2[Cu(H_2O)_2(en)_2]\{[Cu(en)_2(H_2O)]_2Eu(H_2O)_3Te_6Nb_{18}O_{64}(OH)_4\}\cdot 7H_2O$ (***1***). A mixture of $K_7H[Nb_6O_{19}]\cdot 13H_2O$ (0.20 g, 0.146 mmol), $Cu(OAc)_2\cdot H_2O$ (0.12 g, 0.60 mmol), $Eu(NO_3)_3\cdot 6H_2O$ (0.10 g, 0.22 mmol), TeO_2 (0.08 g, 0.50 mmol), pyridine-2,3-dicarboxylic acid (0.03 g, 0.18 mmol), 0.20 ml 2M NaOH and 0.11 ml en was mixed in 6 ml deionized water. After stirred 1 hour, the resulting mixture was sealed in a glass vial (20 ml) and heated at 90 ℃ for 3 days, and then cooled down to room temperature. The blue purple block crystals were isolated. Yield: 15 mg (4.6% based on Nb). Elemental analysis calcd (%) for $H_{121}C_{20}N_{20}Cu_5EuTe_6Nb_{18}O_{84}$: C 4.90, H 2.49, N 5.72. Found (%): C 4.43, H 2.55, N 6.23. IR (KBr, cm^{-1}): 3221(s), 3133(s), 2952(w), 2891(w), 1639(w), 1586(s), 1461(m), 1394(w), 1370(w), 1325(w), 1280(m), 1185 (w), 1106(m), 1041(s), 985(w), 842(s), 688(m), 617(m), 498(m), 427(w).

Synthesis discussion

In the synthesis process, the following reaction parameters show important impacts on the synthesis of **1**:

(1) The temperature of hydrothermal reactions is one of the important factors for the synthesis of the compound **1**. The compound **1** was obtained at 90℃. When the reaction temperature is above or below the 90℃, the yield will decrease dramatically and only amorphous phases would be obtained. (2) We tried to introduce different 3d metals salts (e.g., Co^{2+}, Ni^{2+} and Zn^{2+}) into the reaction instead of Cu^{2+}. However, we failed to obtain any other crystalline HPONb products. (3) The 2M NaOH aqueous solution and pyridine-2, 3-dicarboxylic acid are indispensable for adjusting the pH, when we changed the solvent to other buffer solutions (e.g., $Na_2CO_3/NaHCO_3$ and $Na_2B_4O_7/H_3BO_3$), only amorphous precipitation instead of crystals could be obtained despite their absence in the component.

Single-Crystal Structure Analysis. Single-crystal X-ray diffraction data of **1** were collected on Bruker APEX Due CCD diffractometer equipped with a fine focus, 2.0 kW sealed tube X-ray source (MoKα radiation, λ = 0.71073 Å) operating at 150(2) K. The structure of **1** was solved through direct methods and refined by full-matrix least-squares refinements based on *F2* adopting the SHELX-2014 program package.[20] The contribution of disordered solvent molecules to the overall intensity data of structures were treated using the SQUEEZE method in PLATON.[21] Crystallographic data and structure refinements for **1** are summarized in Table S1. CCDC 2156753 contains supplementary

crystallographic data for this paper. These data can be obtained free of charge from The Cambridge Crystallographic Data Centre via www.ccdc.cam.ac.uk/data_request/cif.

Water adsorption measurement: As-synthesized sample **1** was exchanged with excessive ethanol 9 times for 3 days. The solvent exchanged sample was then degassed at 80 ºC for 12 h under high dynamic vacuum. Water sorption isotherm was recorded at 298K on a micromeritics 3flex Adsorption Analyzer.

The reactivity test of compound 1:

Firstly, HCl and NaOH compounds were used to prepare aqueous solutions with pH 1-14, and then 20 mg of compound **1** was added to 5 mL of aqueous solutions with different pH values and soaked for 24 hours, respectively. Finally, the soaked crystals were taken out and tested for PXRD. The compound **1** was insoluble in the aqueous solutions with different pH values. The compound **1** which had been soaked for 24 hours was filtrated, washed with water and dried under vacuum at room temperature.

20 mg of compound **1** was added to a 5 mL of organic solvent and soaked for 24 hours. Then the soaked crystals were taken out and tested for PXRD. The compound **1** was insoluble in the organic solvents. The compound **1** which had been soaked for 24 hours was filtrated, washed with water and dried under vacuum at room temperature.

Proton conductivity experiments: Ac impedance measurements were carried out with a SI 1260 IMPEDANCE/GAINPHASE analyzer over the frequency range from 0.1 Hz to 10 MHz with an applied voltage of 50 mV. The relative humidity was controlled by a STIK Corp CIHI-150BS3 incubator. The samples were pressed to form a cylindrical pellet of crystalline powder sample (~1 mm thickness ×5 mm ϕ) coated with C-pressed electrodes. Two silver electrodes were attached to both sides of pellet to form four end terminals (quasi-four-probe method). The bulk conductivity was estimated by semicircle fittings of Nyquist plots.

Section 2: Additional tables

Table S1 Crystal data and structure refinement for **1**.

	1
Empirical formula	$H_{121}C_{20}N_{20}Cu_5EuTe_6Nb_{18}O_{84}$
Formula weight	4893.68
Crystal system	Monoclinic
space group	$P2_1/m$
a (Å)	13.7123(7)
b (Å)	34.3657(15)
c (Å)	19.9008(10)
B(°)	92.736(2)
V (Å^3)	9367.2(8)
Z	2
F(000)	4622
ρcalcd (g·cm^{-3})	1.735
Temperature (K)	150
Refl. Collected	184527
Independent relf.	16908
Parameters	706
GOF on F^2	1.067
Final *R* indices ($I= 2\sigma(I)$)	R_1= 0.0541 wR_2= 0.1372
R indices (all data)	R_1= 0.0610 wR_2= 0.1415

$R_1 = \sum||F_o| - |F_c||/\sum|F_o|$. $wR_2 = [\sum w(F_o^2 - F_c^2)^2/\sum w(F_o^2)^2]^{1/2}$; $w = 1/[\sigma^2(F_o^2) + (xP)^2 + yP]$, $P = (F_o^2 + 2F_c^2)/3$, where x = 0.061200, y = 105.458809 for **1**.

Table S2. Hydrogen Bond Lengths (Å) and Bond Angles (°) in **1**.

No.	N-H	H···O	N···O	<(NHO)	Hydrogen bonds
1	0.89	2.47	3.211(12)	140.5	N1-H1A···O12
2	0.89	2.63	3.308(13)	133.7	N1-H1A···O33
3	0.89	1.98	2.863(11)	172.1	N2-H2A···O21_$3
4	0.89	2.33	3.184(10)	160.9	N2-H2B···O30
5	0.89	2.26	3.140(12)	171.7	N3-H3A···O7W
6	0.89	2.12	2.956(11)	156.2	N3-H3B···O33
7	0.89	2.16	3.005(11)	157.5	N4-H4A···O37
8	0.89	2.27	3.071(9)	149.6	N4-H4B···O11_$3
9	0.89	2.09	2.956(11)	164.7	N5-H5B···O31_$4
10	0.89	2.24	3.088(10)	158.5	N6-H6A···O25_$4
11	0.89	2.19	3.074(10)	173.0	N7-H7A···O4
12	0.89	2.50	2.944(10)	111.4	N7-H7A···O13
13	0.89	2.26	3.073(9)	151.7	N7-H7B···O2
14	0.89	2.16	3.028(10)	163.7	N8-H8A···O17
15	0.89	2.34	3.199(11)	163.7	N8-H8B···O29
6	0.89	2.23	3.081(10)	160.2	N9-H9A···O33
17	0.89	2.14	3.022(9)	168.7	N9-H9B···O17
18	0.89	2.31	3.155(9)	159.0	N10-H10A···O6
19	0.89	2.23	3.106(10)	169.7	N10-H10B···O32
Symmetric codes: $3: x-1, y, z. $4: -x+2, -y+1, -z.					

Table S3. A summary of known vapour adsorption capacities of polyoxometalate materials.

Compounds	Amount ($cm^3 \bullet g^{-1}$)	ref
1	167	This work
$\{[Cu(en)_2]_6[Nb_{68}O_{176}(OH)_{12}(H_2O)_{12}]\}$	172	S1
$\{[Cu(en)_2]_{10}[Nb_{68}O_{182}(OH)_8\ (H_2O)_{10}]\}$	140	S1
$[Cu(en)_2(H2O)]_2\{[Cu(en)]_4[Cu(en)_2]_5[Cu(en)_2KNb_{24}O_{72}H_{10}]_2\}$	204	S2
$[Cu(en)_2]_6\{[Cu(en)_2]@\{[Cu_2\,(trz)_2(en)_2]_6[H_{10}Nb_{68}O_{188}]\}\}$	224	S3
$K_4@\{[Cu_{29}(OH)_7(H_2O)_2(en)_8(trz)_{21}][Nb_{24}O_{67}(OH)_2(H_2O)_3]_4\}$	193	S3
$[Cu(en)_2]@\{[Cu_2(en)_2(trz)_2]_6(Nb_{68}O_{188})\}$	188	S3
$[Zn_{12}(trz)_{20}][SiW_{12}O_{40}]\cdot 11H_2O$	150	S4
$K_3[Cr_3O(OOCH)_6(H_2O)_3][R\text{-}SiW_{12}O_{40}]$	130	S5
$Cu_6(Trz)_{10}(H_2O)_4[H_2SiW_{12}O_{40}]\cdot 8H_2O$	118	S6
$[Cu_4(dpdo)_{12}][H(H_2O)_{27}(CH_3CN)_{12}][PW_{12}O_{40}]_3$	65.1	S7
$K_2[Cr_3O(OOCH)_6(mepy)_3]_2[\alpha\text{-}PMo_{12}\ O_{40}]\cdot 5H_2O$	56.8	S8
$H_{14}[Na_6(H_2O)_{12}]_4[K_{42}Ge_8W_{72}O_{272}(H_2O)_{60}]\cdot$solvent	52	S9
$[Cu_3(L)_2(H_2O)_4][Cu(dmf)_4\ (SiW_{12}O_{40})]\cdot 9H_2O$	51.7	S10
$H[Ni(Hbpdc)(H_2O)_2]_2[PW_{12}O_{40}]\cdot 8H_2O\}$	31	S11
$[Co(pn)_3]_4[PNb_{12}O_{40}(VO)_6][OH]_5\cdot 20H_2O$	19.72	S12
$(DODA)_{23}[Mo_{154}O_{462}H_5]\cdot 70H_2O$	16.6	S13
$Cs_{3.6}K_{0.4}[PW_{11}O_{39}(Sn\text{-}OH)]\cdot 8H_2O$	0.31	S14
$K_2[Cr_3O(OOCH)_6(mepy)_3]_2[a\text{-}SiW_{12}O_{40}]\cdot 2H_2O\cdot CH_3OH$	0.03	S15
$Cs_2[Cr_3O(OOCC_2H_5)_6(H_2O)_3]_2\ [R\text{-}SiW_{12}O_{40}]\cdot 4H_2O$	0.022	S16,S17
$Cs_3H_{0.3}[SiW_{12}O_{40}]_{0.83}\cdot 3H_2O$	0.020	S18

[a] Trz: 1,2,4-triazole; dpdo: 4,4'-bipyridine-N,N'-dioxide; mepy: 4-methylpyridine; L: *N*,*N*-bis[(2-hydroxy-3-methoxyphenyl) methylidene] hydrazine hydrate ; dmf: N,N-Dimethylformamide; H_2bpdc : 2,2'-bipyridyl-3,3'-dicarboxylicacid; pn: 1,2-diaminopropane; DODA: dimethyldioctadecyl

ammonium.

Section 3: Additional structural figures and characterizations

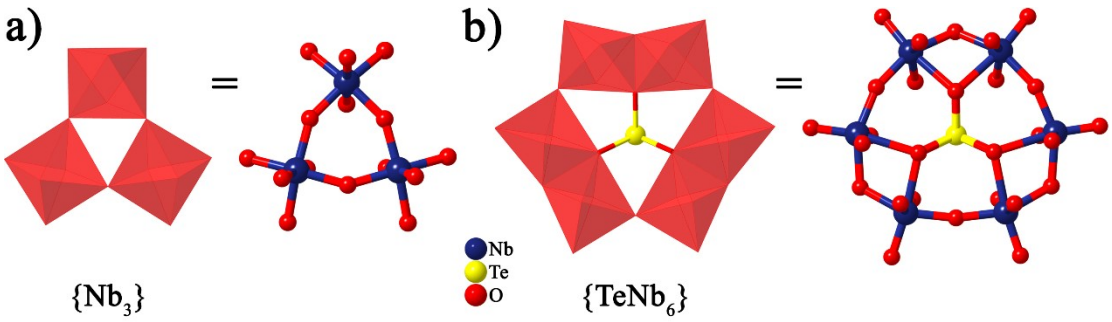

Fig S1. (a) Polyhedral and ball-stick representations of { Nb_3O_4} unit in **1**; (b) Polyhedral and ball-stick representations of {$TeNb_6$}unit in **1**. Color code: Nb:blue; Te: yellow; O: red.

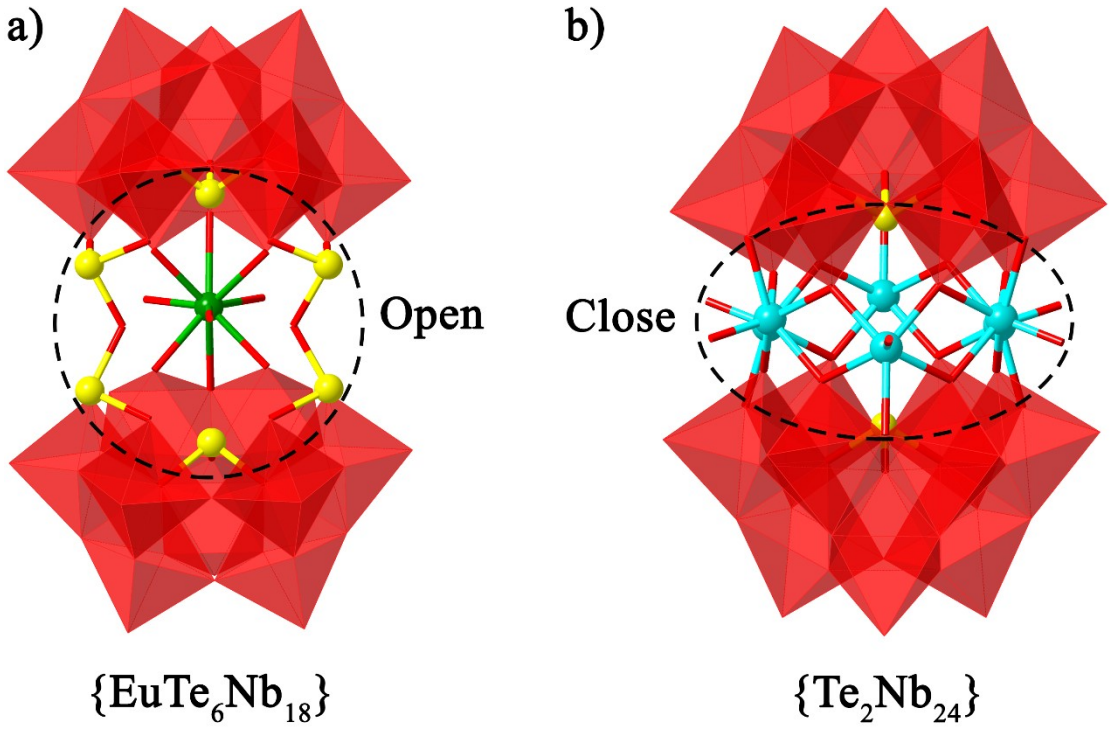

Fig S2. (a) Side view of {$EuTe_6Nb_{18}$} in **1**; (b) Side view of {Te_2Nb_{24}} in **1**. Color code: Nb: cyan; Eu: green; Te: yellow.

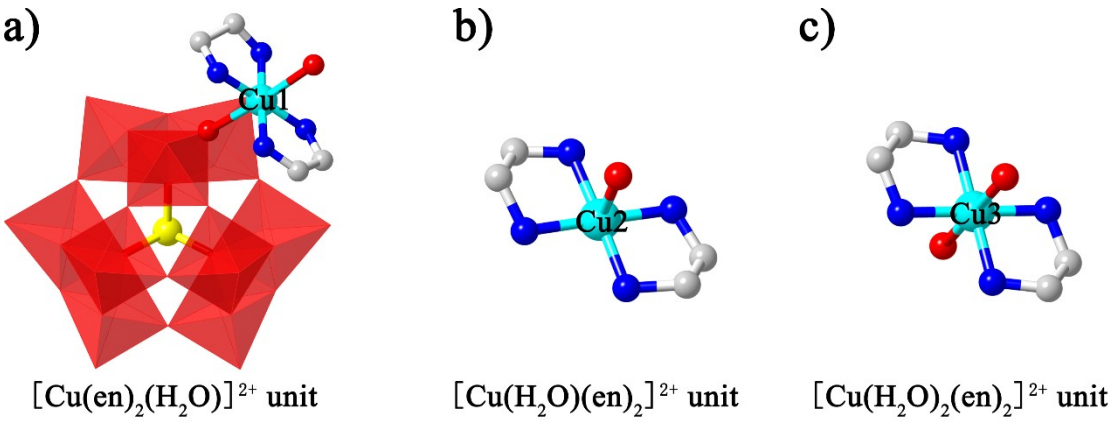

Fig S3. Coodination environments of $[Cu(en)_2(H_2O)]^{2+}$ (Cu1) unit in **1** (a); $[Cu(H_2O)(en)_2]^{2+}$ (Cu2) (b); unit $[Cu(H_2O)_2(en)_2]^{2+}$ (Cu3) (c). Color code: Cu: cyan; Te: yellow. C: grey; N: blue; O: red.

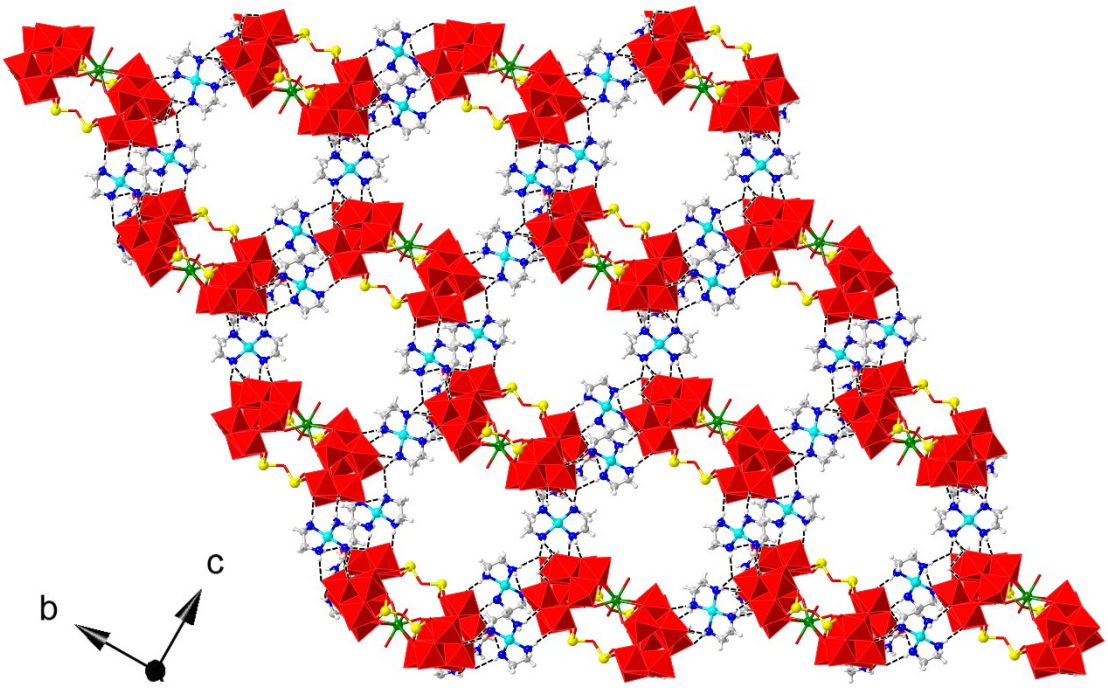

Fig S4. View of a 2D supramolecular (4, 4) layer in the *bc* plane in **1**. Color code: Cu: cyan; Eu: green; Te: yellow. C: grey; N: blue.

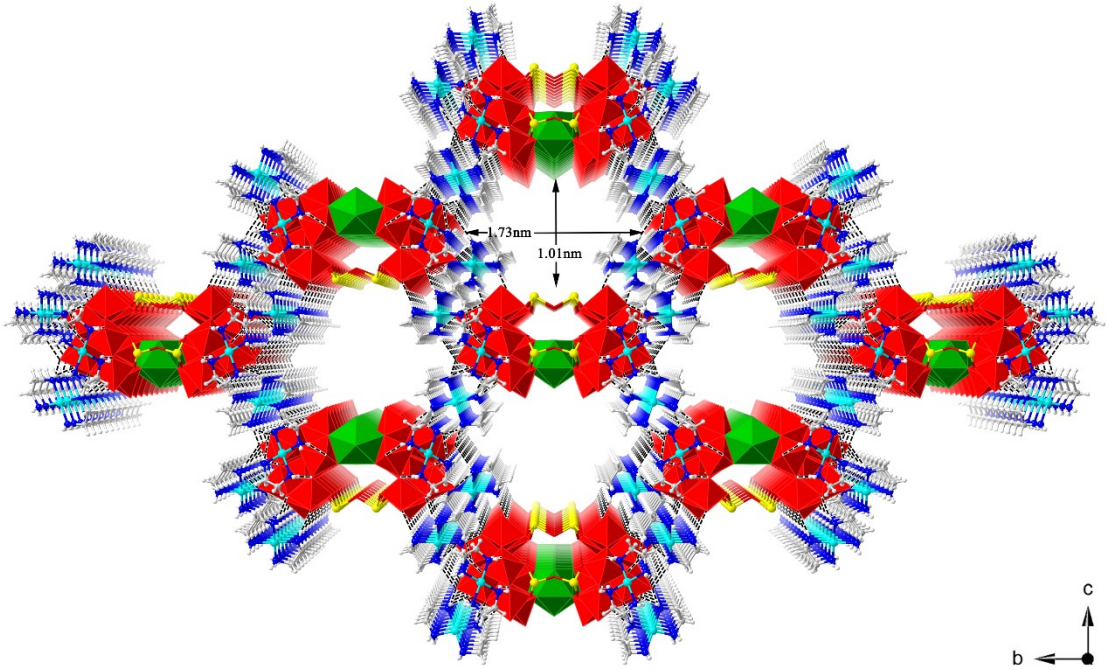

Fig S5. View of the three-dimensional supramolecular framework of **1** along the *a* axis. Color code: Cu: cyan; Te: yellow. C: grey; N: blue.

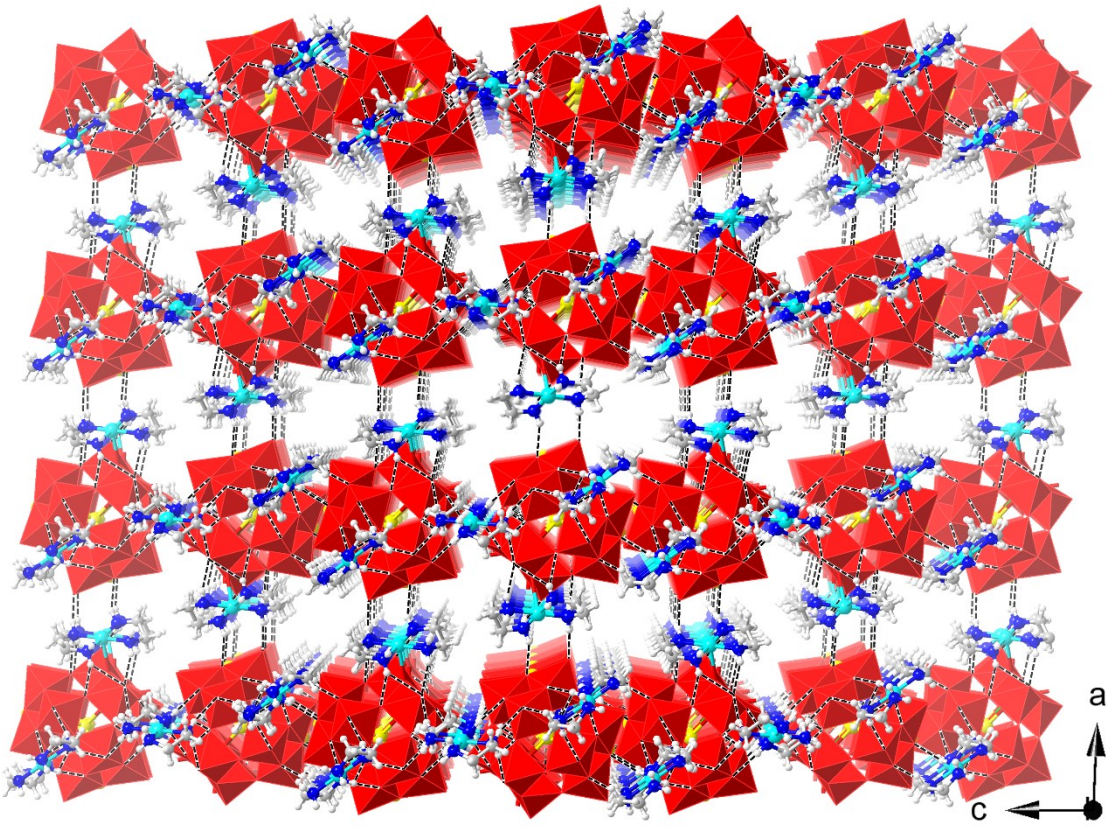

Fig S6. View of the three-dimensional supramolecular framework of **1** along the *b* axis. Color code: Cu: cyan; Te: yellow. C: grey; N: blue.

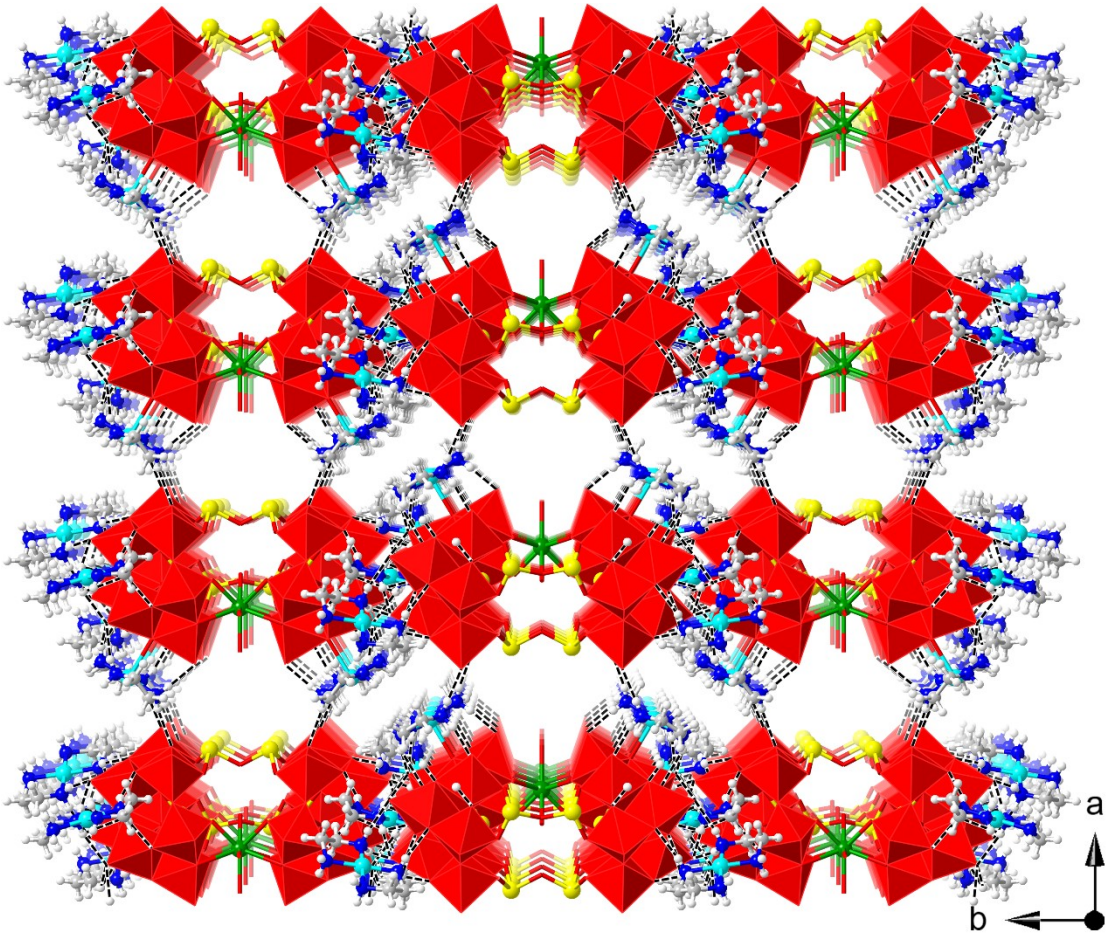

Fig S7. View of the three-dimensional supramolecular framework of **1** along the *c* axis. Color code: Cu: cyan; Te: yellow. C: grey; N: blue.

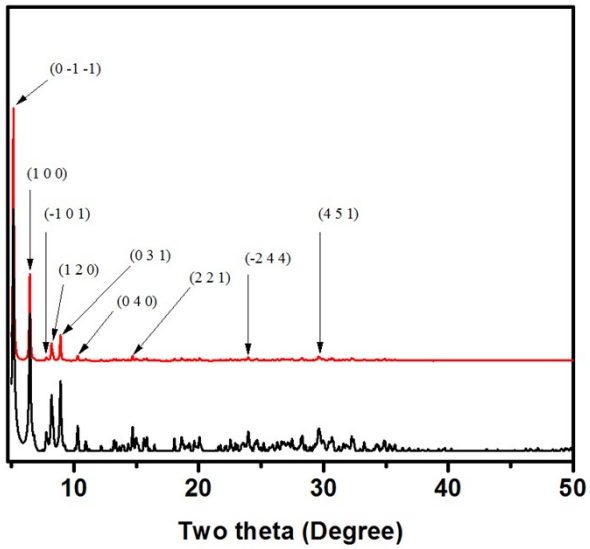

Fig S8. The simulated and experimental PXRD patterns of **1**.

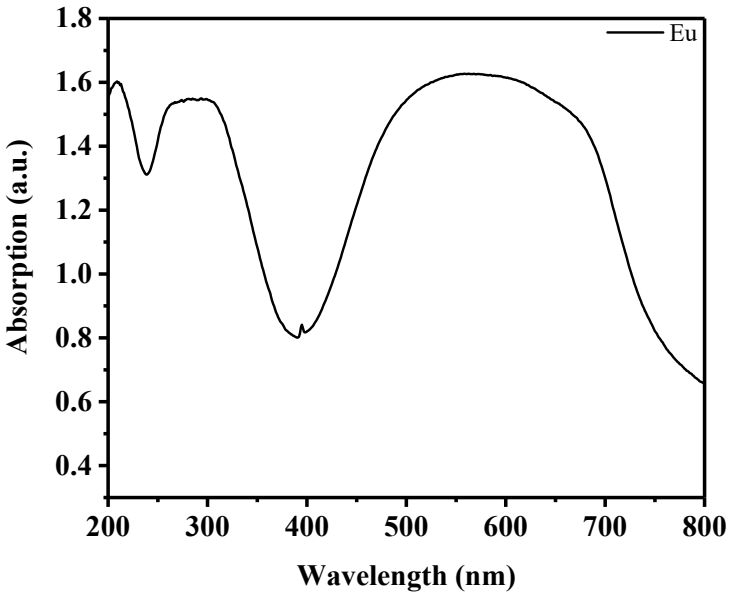

Fig S9. Plot of UV-vis absorption spectrum of **1**.

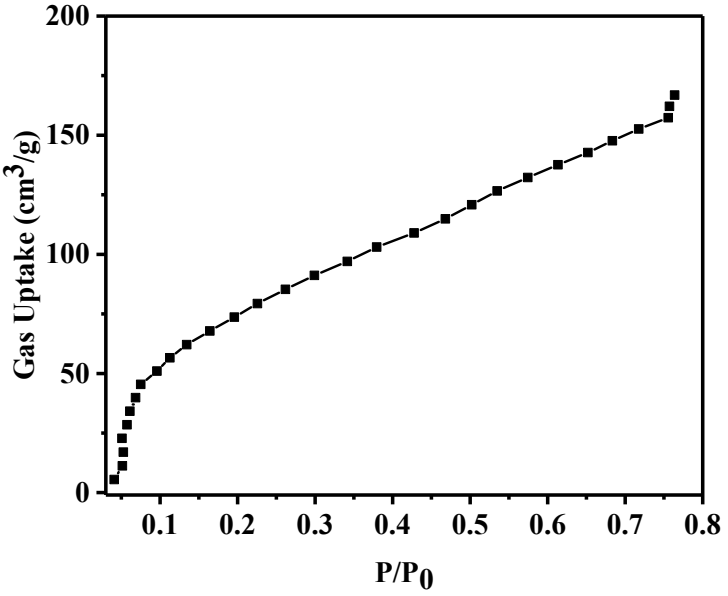

Fig S10. Water vapor adsorption curve of **1** at 298 K.

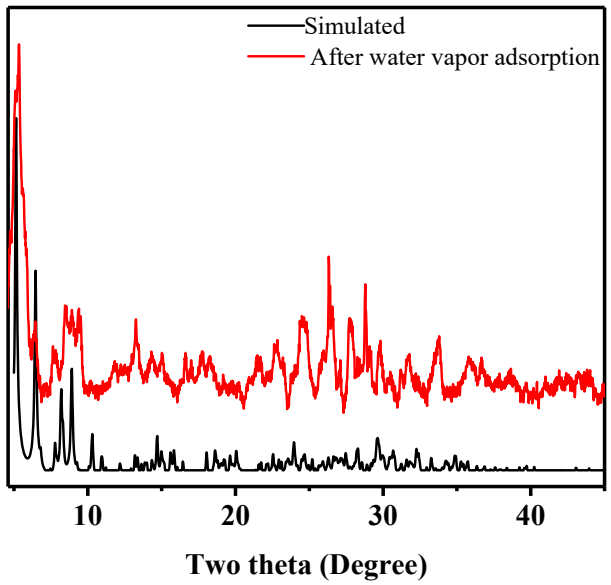

Fig S11. PXRD patterns of **1** after water vapor adsorption experiment.

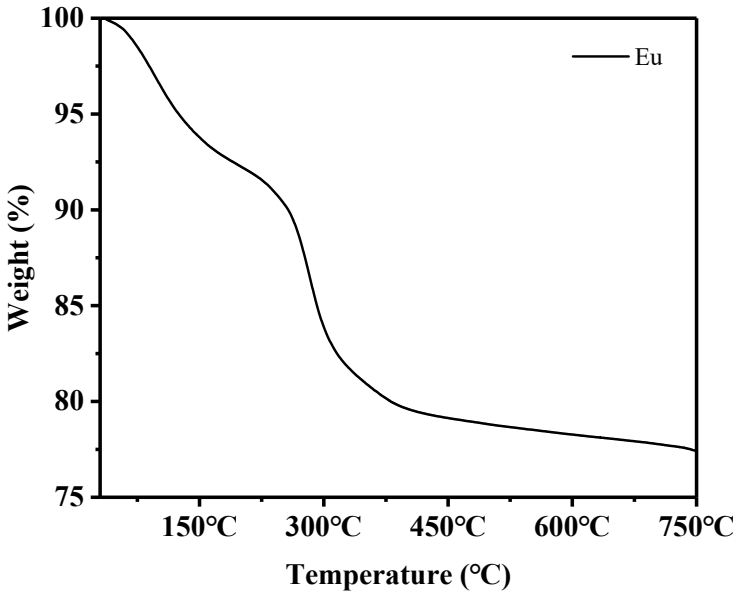

Fig S12. TGA curve of **1**.

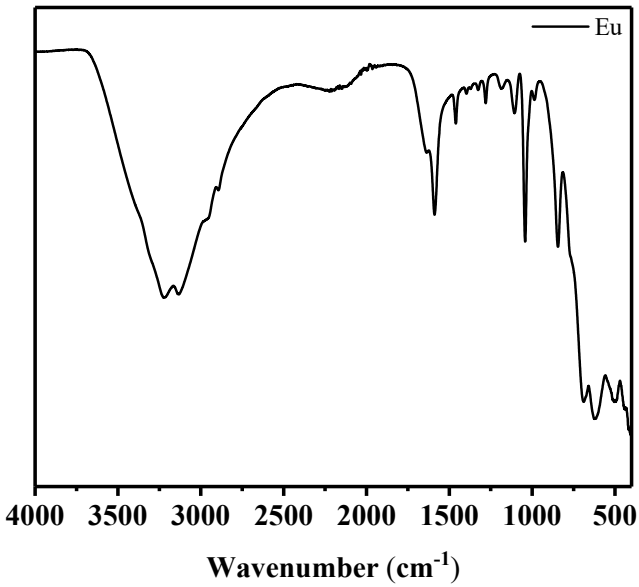

Fig S13. IR spectrum of **1**.

As shown in Figure S13, the O-H, C-H and N-H stretching vibration bands are observed at $\tilde{\nu}$ = 2800 to 3300 cm^{-1}, and their bending vibration bands are observed at $\tilde{\nu}$ = 1100-1600 cm^{-1}. The characteristic peaks at $\tilde{\nu}$ = 1041, 985, 842, 688, 617, 498, and 427 cm^{-1} are assigned to the ν(Nb-O_t) and ν(Nb-O_b-M) stretches (M = Nb, Cu).

Section 4: Topology analysis

Topology for Eu1

Atom Eu1 links by bridge ligands and has

Common vertex with					R(A-A)	
Eu 1	1.8729	0.7500	0.3143	(1 0 0)	13.712A	1
Eu 1	-0.1271	0.7500	0.3143	(-1 0 0)	13.712A	1
Eu 1	1.1271	1.2500	0.6857	(2 0 1)	18.962A	1
Eu 1	1.1271	0.2500	0.6857	(2-1 1)	18.962A	1
Eu 1	1.1271	1.2500	-0.3143	(2 0 0)	21.635A	1
Eu 1	1.1271	0.2500	-0.3143	(2-1 0)	21.635A	1

Structural group analysis

Structural group No 1

Structure consists of 3D framework with Eu

Coordination sequences

Eu1:	1	2	3	4	5	6	7	8	9	10
Num	6	18	38	66	102	146	198	258	326	402
Cum	7	25	63	129	231	377	575	833	1159	1561

Rad 18.1(3.6) 28.8(7.3) 40.1(10.1) 51.9(12.4) 64.0(14.9) 76.2(17.4) 88.5(19.9) 100.8(22.5) 113.2(25.1) 125.5(27.7)

Cmp Eu6 Eu18 Eu38 Eu66 Eu102 Eu146 Eu198 Eu258 Eu326 Eu402

TD10=1561

Vertex symbols for selected sublattice

Eu1 Point symbol:{4^12.6^3}

Extended point symbol:[4.4.4.4.4.4.4.4.4.4.4.4.6(4).6(4).6(4)]

Point symbol for net: {4^12.6^3}

6-c net; uninodal net

Section 4: References

[1] Lin, Y,-D.; Zhu, Z,-K.; Ge, R.; Yu, H.; Li, Z.; Sun, C.; Sun,Y.-Q.; Li, X.-X.; Zheng, S.-T. Proton conductive polyoxoniobate frameworks constructed from nanoscale $\{Nb_{68}O_{200}\}$ cages. *Chem. Commun.*, **2021**, 57, 4702–4705.

[2] Zhu, Z.-K.; Lin, L.-D.; Zhang, J.; Li, X.-X.; Sun,Y.-Q.; Zheng, S.-T. A rare 4-connected neb-type 3D chiral polyoxometalate framework based on $\{KNb_{24}O_{72}\}$ clusters. s: *Inorg. Chem. Front*., **2020**, 7, 3919–3924.

[3] Zhu, Z.-K.; Lin, Y.-Y.; Yu, H.; Li, X.-X. Zheng, S.-T. Inorganic‑Organic Hybrid Polyoxoniobates: Polyoxoniobate Metal Complex Cage and Cage Framework. *Angew. Chem. Int. Ed.* **2019***, 58,* 16864-16868.

[4] Zhou, E.-L.; Qin, C.; Wang, X.-L.; Shao, K.-Z. Su, Z.-M. Steam-Assisted Synthesis of an Extra-Stable Polyoxometalate-Encapsulating Metal Azolate Framework: Applications in Reagent Purification and Proton Conduction. *Chem. Eur. J.* **2015**, *21*, 13058-13064.

[5] Uchida, S.; Kawamoto, R.; Mizuno, N. Recognition of Small Polar Molecules with an Ionic Crystal of α-Keggin-Type Polyoxometalate with a Macrocation. *Inorg. Chem.* **2006**, *45*, 5136-5144.

[6] Zhou, E.-L.; Qin, C.; Huang, P.; Wang, X.-L.; Chen, W.-C.; Shao, K.-Z.; Su, Z.-M. A Stable Polyoxometalate-Pillared Metal–Organic Framework for Proton-Conducting and Colorimetric Biosensing. *Chem. Eur. J.* **2015**, *21*, 11894-11898.

[7] Wei, M.; Chen, L.; Duan, X. A porous Cu(II)-MOF containing $[PW_{12}O_{40}]^{3-}$ and a large protonated water cluster: synthesis, structure, and proton conductivity. *J. Coord. Chem.* **2014**, *67*, 2809-2819.

[8] Kawahara, R.; Uchida, S.; Mizuno, N. Redox-Induced Reversible Uptake−Release of Cations in Porous Ionic Crystals Based on Polyoxometalate: Cooperative Migration of Electrons with Alkali Metal Ions. *Chem. Mater.* **2015**, *27*, 2092-2099.

[9] Li, Z.; Lin, L.-D.; Yu, H.; Li, X.-X. Zheng, S.-T. All-Inorganic Ionic Porous Material Based on Giant Spherical Polyoxometalates Containing Core-Shell K_6@K_{36}-Water Cage. *Angew. Chem. Int. Ed.* **2018**, *57*, 15777-15781.

[10] Wei, M.-L.; Sun, J.-J.; Duan, X.-Y. A Complex Based on a CuII–Schiff-Base Complex and POM-MOF Chain: Synthesis, Structure and Proton Conductivity. *Eur. J. Inorg. Chem.* **2014**, 345-351.

[11] Wei, M.; Wang, X.; Sun, J.; Duan, X. A 3D POM–MOF composite based on Ni(II) ion and 2,2′-bipyridyl-3,3′-dicarboxylic acid: Crystal structure and proton conductivity. *J. Solid State Chem.* **2013**, *202,* 200-206.

[12] Hu, J.; Xu, Y.; Zhang, D.; Chen, B.; Lin, Z.; Hu, C. A Highly Symmetric Ionic Crystal Constructed by Polyoxoniobates and Cobalt Complexes for Preferential Water Uptake over Alcohols. *Inorg. Chem.* **2017**, *56*, 10844-10847.

[13] Noro, S.; Tsunashima, R.; Kamiya, Y.; Uemura, K.; Kita, H.; Cronin, L.; Akutagawa, T.; Nakamura, T. Adsorption and Catalytic Properties of the Inner Nanospace of a Gigantic Ring-Shaped Polyoxometalate Cluster. *Angew. Chem. Int. Ed.* **2009**, *48*, 8703-8706.

[14] Miura, Y.; Imai, H.; Yokoi, T.; Tastumi, T.; Kamiya, Y. Microporous cesium salts of tetravalent Keggin-type polyoxotungstates $Cs_4[SiW_{12}O_{40}]$, $Cs_4[PW_{11}O_{39}(Sn\text{-}n\text{-}C_4H_9)]$, and $Cs_4[PW_{11}O_{39}(Sn\text{-}OH)]$ and their adsorption properties. *Microporous Mesoporous Mater*. **2013**, *174*, 34-43.

[15] Uchida, S.; Eguchi, R.; Mizuno, N. Zeotype Organic‑Inorganic Ionic Crystals: Facile Cation Exchange and Controllable Sorption Properties. *Angew. Chem. Int. Ed.* **2010**, *49*, 9930-9934.

[16] Lesbani, A.; Kawamoto, R.; Uchida, S.; Mizuno, N. Control of Structures and Sorption Properties of Ionic Crystals of $A_2[Cr_3O(OOCC_2H_5)_6(H_2O)_3]_2[\alpha\text{-}SiW_{12}O_{40}]$ (A = Na, K, Rb, NH_4, Cs, TMA). *Inorg. Chem.* **2008**, *47*, 3349-3357.

[17] Jiang, C.; Lesbani, A.; Kawamoto, R.; Uchida, S.; Mizuno, N. Channel-Selective Independent Sorption and Collection of Hydrophilic and Hydrophobic Molecules by $Cs_2[Cr_3O(OOCC_2H_5)_6(H_2O)_3]_2[\alpha\text{-}SiW_{12}O_{40}]$ Ionic Crystal. *J. Am. Chem. Soc.* **2006**, *128*, 14240-14241.

[18] Ogasawara, Y.; Uchida, S.; Maruichi, T.; Ishikawa, R.; Shibata, N.; Ikuhara, Y.; Mizuno, N. Cubic Cesium Hydrogen Silicododecatungstate with Anisotropic Morphology and Polyoxometalate Vacancies Exhibiting Selective Water Sorption and Cation-Exchange Properties. *Chem. Mater.* **2013**, *25*, 905-911.

[19] M. FILOWITZ, R. K. C. HO, W. G. KLEMPERER, and W. SHUM. Oxygen-17 nuclear magnetic resonance spectroscopy of polyoxometalates. 1. Sensitivity and resolution. *Inorg. Chem*., **1979**, 18, 93-103.

[20] Sheldrick, G. M. A Short History of SHELX. *Acta Crystallogr., Sect. A: Found. Crystallogr.* **2008**, *64*, 112-122.

[21] Spek, A. L. Single-crystal Structure Validation with the Program PLATON. *J. Acta Crystallogr.* **2003**, *36*, 7-13.